[6] Lutz, E., et al. (1991)
The land mobile satellite communications channel—recording, statistics, and channel model.
IEEE Transactions on Vehicular Technology, **40**, 2 (May 1991), 375–386.

[7] Korn, I. (1992)
Error probability of digital modulation in satellite mobile, land mobile, and Gaussian channels with narrow-band receiver filter.
IEEE Transactions on Communications, **40**, 4 (Apr. 1992), 697–707.

[8] Nelson, N. T. (1994)
Probability of bit error on a standard IRIG telemetry channel using the aeronautical fading channel model.
In *Proceedings of the International Telemetering Conference*, San Diego, CA, **30** (Oct. 1994), 356–363.

[9] Balanis, C. A. (1989)
Advanced Engineering Electromagnetics.
New York: Wiley, 1989.

[10] Rice, M., and Friend, D. (1997)
Antenna gain pattern effects on multipath interference in aeronautical telemetering.
In *Proceedings of the International Telemetering Conference*, Las Vegas, NV, **33** (1997), 113–120.

[11] Sutton, R., Schroeder, E., Thompson, A., and Wilson, S. (1973)
Satellite-aircraft multipath and ranging experiment results at L-band.
IEEE Transactions on Communications, **COM-21**, 5 (May 1973), 639–647.

[12] Rummler, W. D. (1979)
A new selective fading model: Application to propagation data.
Bell System Technical Journal, **58**, 5 (May–June 1979), 1037–1071.

[13] Vucetic, B., and Du, J. (1992)
Channel modeling and simulation in satellite mobile communication systems.
IEEE Journal on Selected Areas in Communications, **10**, 8 (Oct. 1992), 1209–1218.

[14] Parsons, J. D. (1994)
The Mobile Radio Propagation Channel.
New York: Wiley, 1994.

[15] Young, W. R., and Lacy, L. Y. (1950)
Echoes in transmission at 450 megacycles from land-to-car radio units.
Proceedings of the IRE, **38** (1950), 255–258.

[16] Turin, G. L., Clapp, F. D., Johnston, T. L., Fine, S. B., and Lavry, D. (1972)
A statistical model of urban multipath propagation.
IEEE Transactions on Vehicular Technology, **VT-21**, 1 (1972), 1–9.

[17] Cox, D. C. (1972)
Delay-Doppler characteristics of multipath propagation at 910 MHz.
IEEE Transactions on Antennas and Propagation, **AP-20**, 9 (Sept. 1972), 625–635.

[18] Range Commanders Council Telemetry Group (1993)
IRIG Standard 106-93: Telemetry Standards.
Range Commanders Council, White Sands Missile Range, New Mexico, 1993.

[19] Papoulis, A. (1984)
Probability, Random Variables, and Stochastic Processes (2nd ed.).
New York: McGraw-Hill, 1984.

[20] Divsalar, D. (1991)
Calculation of Rician parameter for AMT.
Interoffice memorandum AMT:331.2-90-078, Jet Propulsion Laboratory, Pasadena, CA, Feb. 1991.

[21] Dye, R. (1996)
Signal strength analysis of angle modulated data in the presence of multipath fading.
M.S. thesis, Brigham Young University, Provo, UT, 1996.

[22] Horne, L., and Dye, R. (1995)
An inexpensive data acquisition system for measuring telemetry signals on test ranges to estimate channel characteristics.
In *Proceedings of the International Telemetering Conference*, Las Vegas, NV, **31** (Oct. 1995), 210–215.

[23] Hill, E. R. (1973)
Time domain analysis of an automatic gain control weighted diversity combining system.
Technical report TP-73-74, Pacific Missile Test Center, Pt. Mugu, CA, Dec. 1973.

[24] Hill, E. R. (1978)
Techniques and circuits for implementing pre-detection diversity combiners.
Technical report TP-78-20, Pacific Missile Test Center, Pt. Mugu, CA, Sept. 1978.

Performance Assessment of CFAR Processors in Pearson-Distributed Clutter

An analytical study on the performance of three existing classes of constant false alarm rate (CFAR) detectors operating in heavy tailed distributed data is presented. In particular, we study the performance of the cell averaging (CA), order statistics (OS), and p-percent truncated mean (PTM) CFAR processors when the output measurements of the square-law detector can be modeled as positive alpha-stable ($P\alpha S$) random variables with a shape parameter (characteristic exponent) equal to 0.5. We derive the exact expressions for the detection and false alarm probabilities of the detectors, and compare their performance by means of their corresponding receiver operating characteristics (ROC).

I. INTRODUCTION

In radar systems, target detection involves the comparison of the absolute value (linear detector)

Manuscript received March 28, 1999; revised October 25, 1999 and March 25 and May 19, 2000; released for publication June 20, 2000.

IEEE Log No. T-AES/36/4/11383.

Refereeing of this contribution was handled by L. M. Kaplan.

This work was supported by the Carderock Division of the Naval Surface Warfare Center's In-house Laboratory Independent Research Program sponsored by the Office of Naval Research and administrated by the Research Director, Code 0112 under Program Element 061152N under NSWCCD Contract N00167-96-M3140. The work of the first author was also supported by the Greek General Secretariat for Research and Technology under Program ΕΠΕΤ II, Code 97ΕΛ-152.

or the squared magnitude (square-law detector) of the coherent receiver output signals with a certain threshold. It is extremely important for the detection radar to be able to operate in nonstationary background noise environments with a predetermined constant level of performance. In signal processing terms, the goal is to maintain a constant false alarm rate (CFAR) when the background noise level fluctuates.

It is impossible to maintain CFAR performance in nonstationary environments with a detection scheme that employs a fixed threshold. Hence, CFAR detectors have been designed that set the threshold adaptively according to local information on the background noise. More specifically, CFAR detectors estimate characteristics of the noise, such as its shape and scale, by processing a window of reference cells surrounding the cell under test in range and/or frequency.

The cell averaging (CA) approach is such an adaptive procedure. The CA CFAR detector uses the maximum likelihood estimate of the noise power to set the threshold adaptively on the assumption that the background noise amplitude samples are independent, identically distributed (IID) random variables with a Rayleigh probability density function (pdf). The CA CFAR detector is the optimum CFAR detector in terms of detection probability in homogeneous noise background with Rayleigh statistics [1].

However, the assumption of a uniform clutter situation within the reference window is hardly ever maintained in practice due to transitions in clutter characteristics, clutter areas of small extensions, and interfering target echoes occurring within the reference window of the radar test cell. Because the performance of the CA CFAR detector degrades considerably in nonhomogeneous situations, Rohling modified the common CA CFAR technique by replacing the arithmetic averaging estimator of clutter power with a new module based on order statistics (OS) [2]. The OS CFAR processor determines the detection threshold based on the ranked reference cells, a procedure that protects against nonhomogeneous situations caused by interfering targets and clutter edges.

Introduced by Rickard and Dillard as a compromise between the CA and OS processor, the so-called *p-percent truncated mean* (PTM) processor is defined as the arithmetic mean of the first p-percent of the ranked observations [3]. This type of detector is also known as the *censored mean-level detector* and its CFAR performance has been studied by Ritcey in a multiple-target environment when a fixed number of Swerling II targets are present [4].

The performance comparison of the various CFAR procedures in a homogeneous noise background is based on the corresponding relative "additional detectability loss" or "CFAR loss." Naturally, the false alarm probability is a function of the threshold but it also depends on the assumed statistics of the underlying noise. In many situations, the Gaussian distribution cannot appropriately model clutter returns whose amplitude distribution is far more impulsive than the one predicted by the Rayleigh law. Today, a number of studies suggest that clutter modeling is more accurately achieved by considering families of density functions, which depend on a scale parameter ruling the clutter "power" and a shape parameter ruling the behavior of the distribution in the high-amplitude tail [5–7]. Hence, it is important to ensure CFAR performance against variations of both parameters, even at a cost of higher CFAR loss than the single-parameter techniques.

The design and performance evaluation of biparametric CFAR processors for Weibull background has been studied in the past. Weber and Haykin have proposed a two-parameter algorithm in which the threshold is obtained from two ranked background samples [8]. To achieve a lower CFAR loss algorithm, Ravid and Levanon used the maximum likelihood method to estimate the shape and scale parameters of the Weibull distribution [9].

Here we assess the performance of CFAR processors operating in heavy-tailed clutter environments whose signal power flow can be modeled according to the so-called positive alpha-stable ($P\alpha S$) family of distributions. $P\alpha S$ processes have been shown to be related to the power or energy flow in many physical processes including radar sea clutter modulation, seismic activity, and ocean waves [10]. In the following, after describing the OS CFAR processor for Rayleigh clutter, we demonstrate the use of OS CFAR processing for the case of the heavy-tailed Pearson (or Lévy) distribution. We show that the OS processor gives indeed rise to a CFAR detector for Pearson-distributed heavy-tailed output signals and we derive the false alarm probability of the resulting system. Then, we study the performance of the CA detector in heavy-tailed clutter and finally, we analyze the performance of the PTM processor in Pearson-distributed data.

II. CFAR PROCESSORS FOR HEAVY-TAILED MEASUREMENTS

Radar detection of a signal in additive noise is often accomplished by constructing and comparing a test statistic with an adaptive threshold equal to a scaled estimate of the noise strength [4]. For a system that square-law detects the output of a matched filter to obtain the test statistic, the problem can be modeled as the following hypothesis testing problem:

$$\begin{aligned} &H_1 \text{ (target present)} : Y = d + g \\ &H_0 \text{ (target absent)} : Y = g \end{aligned} \quad (1)$$

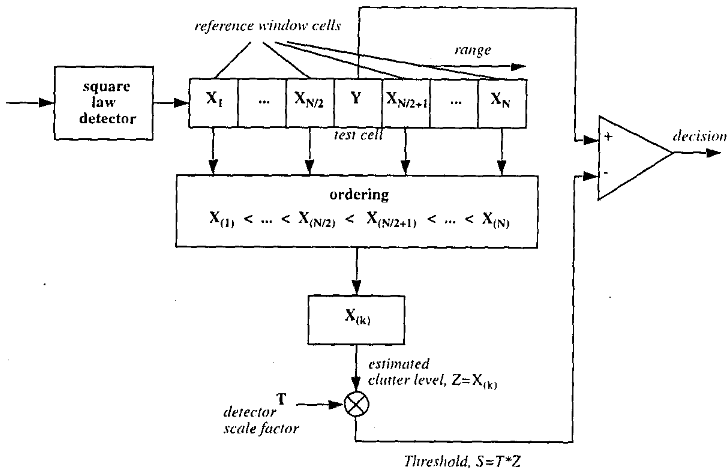

Fig. 1. Block diagram of OS CFAR detector structure.

where d and g are the signal and clutter components, respectively. The signal processing structure is depicted in Fig. 1. Implementing a generalized likelihood ratio test, the decision for H_0 or H_1 is realized by the following thresholding operation:

$$e(Y) = \begin{cases} \text{target present}, & \text{if} \quad Y \geq S \\ \text{target absent}, & \text{if} \quad Y < S \end{cases}. \tag{2}$$

The task of the CFAR system is to provide in an adaptive and systematic manner the threshold value needed. Various CFAR systems are distinguished by the way this threshold is obtained. In existing CFAR systems, target detection is performed by using the sliding window technique. When calculating the threshold, two aspects must be considered. One is the average clutter strength level in the reference window and the other is the required false alarm probability P_{fa}. Accordingly, the threshold S is calculated as the product

$$S = TZ \tag{3}$$

where Z is the estimate of the average clutter strength and T is a scaling factor used to achieve a certain P_{fa}. Different CFAR procedures are characterized by the method used to estimate the clutter level. In the following, we first summarize the OS CFAR results for the case of Rayleigh clutter. Then, we study the OS, CA, and PTM CFAR processors for the case of Pearson-distributed data.

A. OS CFAR for Rayleigh Clutter

Rohling has proposed a CFAR algorithm based on OS that exhibits reduced sensitivity to nonhomogeneous environments as compared with the CA CFAR method. The procedure that takes place in an OS CFAR system is shown in Fig. 1. The data in a reference window around the test cell are used to calculate the decision threshold. The first step is to obtain a measure of the clutter level Z. The N reference cells are ordered according to their magnitude

$$X_{(1)} \leq X_{(2)} \leq \cdots \leq X_{(N-1)} \leq X_{(N)} \tag{4}$$

and Z is taken to be equal to $X_{(k)}$, the kth largest sample. The index k is a parameter in the design of the CFAR detector structure. (As we see in the next subsection, for the case of the CA CFAR processor, Z is the average of the reference window values). The clutter level Z is multiplied by a scaling factor T which depends on the desired false alarm probability for a given window of size N when the background noise is homogeneous. The resulting product TZ is directly used as the threshold value. In practice, the measurements within a certain number of guard cells, directly adjacent to either side of the test cell, are not taken into consideration when estimating Z because signal energy can spill over into the adjacent range cells and may affect the procedure.

When the amplitude samples in the input of the square-law detector are IID random variables with a Rayleigh distribution, then the output samples of the square-law detector $X_1, \ldots, X_N$ follow an exponential distribution. In other words, the exponential density is justified for the output of the square-law detector in the case of complex normally distributed noise in the video range. In this case, Rohling has shown that the relationship between the false alarm probability P_{fa} and the scaling factor T is given by [2]

$$P_{\text{fa}} = \frac{N!(T+N-k)!}{(N-k)!(T+N)!} \tag{5}$$

where k is the representative rank order index and N is the total number of reference window samples. Since (5) is not a function of the scale parameter μ of the noise, the algorithm is CFAR. Rohling points out that a value of k about $3N/4$ is well suited for practical applications.

B. OS CFAR for Pearson-Distributed Data

It is recognized that effective clutter suppression can be achieved only on the basis of appropriate statistical modeling. Actual data, such as active sonar returns [5], sea clutter measurements [10], and monostatic clutter from the US Air Force Mountaintop Database [11], have been successfully modeled with heavy-tailed distributions. The tails of these distributions showed a power-law or algebraic asymptote, which is characteristic of the so-called alpha-stable family and was contrasted with the exponentially decaying tails of the K, and Weibull families. Stable processes are described by their characteristic exponent α, taking values $0 < \alpha \leq 2$ [12, 13]. Because of their algebraic tail property, stable distributions possess finite pth order moments, i.e., $EX^p < \infty$, only when $p < \alpha$. Therefore, stable processes have infinite power.

In this work, we are interested in the totally skewed (positive) alpha-stable ($P\alpha S$) family to describe observed data related to energy, power, and the output of a square-law detector. Unfortunately, closed-form expressions do not exist for the general $P\alpha S$ density except for the case of $\alpha = 0.5$ that defines the Pearson or Lévy distribution. For this main reason, the Pearson is the distribution of interest here. This is further justified by the fact that Pierce showed that the Pearson distribution closely models the modulation or signal power flow of certain see clutter returns [10]. In the following, we study the performance of popular CFAR detectors for the case of Pearson-distributed data by analytically deriving their corresponding receiver operating characteristics (ROCs).

1) *Probability of False Alarm P_{fa}:* Assume that $X_1,\ldots,X_N$ follow the Pearson distribution with pdf [12, p. 10]:

$$p_{X_i}(x) = \begin{cases} \dfrac{\gamma}{\sqrt{2\pi}}\dfrac{1}{x^{3/2}}e^{-\gamma^2/2x}, & x \geq 0 \\ 0 & \text{otherwise} \end{cases} \tag{6}$$

and cumulative density function (cdf)

$$\begin{aligned} P_{X_i}(x) &= \Pr\{X_i \leq x\} \\ &= \begin{cases} 2\left(1-\Phi\left(\dfrac{\gamma}{\sqrt{x}}\right)\right), & x \geq 0 \\ 0 & \text{otherwise} \end{cases} \end{aligned} \tag{7}$$

where γ is the dispersion or scale parameter of the distribution. The dispersion determines the spread of the density, much in the same way that the standard deviation determines the spread of the Rayleigh density. $\Phi(x)$ denotes the cdf of the standard Gaussian distribution $N(0,1)$:

$$\Phi(x) = \int_{-\infty}^{x} \frac{1}{\sqrt{2\pi}}e^{-u^2/2}\,du. \tag{8}$$

With these assumptions, for any given P_{fa} the decision threshold S as well as the scaling factor T can be derived as follows. P_{fa} indicates the probability that a noise random variable Y_0 is interpreted as target echo during the thresholding decision (2). This probability is given by

$$P_{\mathrm{fa}} = \Pr\{Y_0 \geq TZ\}. \tag{9}$$

In order to calculate P_{fa} according to (9), both the pdfs of Y_0 and of Z must be known. Since $Z = X_{(k)}$ is an ordered statistic value, its pdf can be determined based on the pdf, $p_{X_i}(x)$, and the cdf, $P_{X_i}(x)$, of the samples according to [14, pp. 25–26]

$$\begin{aligned} p_{X_{(k)}}(x) = p_k(x) &= \frac{1}{B(k,N-k+1)}[1-P_X(x)]^{N-k} \\ &\quad \times [P_X(x)]^{k-1}p_X(x) \end{aligned} \tag{10}$$

where $B(a,b)$ is the *beta function*. Hence, by using (6), (7), and (10), the pdf of the kth value of the ordered statistic for Pearson-distributed random variables $X_1,\ldots,X_N$ is given by

$$\begin{aligned} p_{X_{(k)}}(x) &= \frac{1}{B(k,N-k+1)}[2\Phi(\gamma/\sqrt{x})-1]^{N-k} \\ &\quad \times 2^{k-1}[1-\Phi(\gamma/\sqrt{x})]^{k-1}\frac{\gamma}{\sqrt{2\pi}}\frac{1}{x^{3/2}}e^{-\gamma^2/2x}. \end{aligned} \tag{11}$$

Now, the P_{fa} can be calculated for a fixed factor T

$$\begin{aligned} P_{\mathrm{fa}} &= \Pr\{Y_0 \geq TX_{(k)}\} = \int_0^\infty \Pr\{Y_0 \geq Tx\}p_k(x)\,dx \\ &= \int_0^\infty [2\Phi(\gamma/\sqrt{Tx})-1]\frac{1}{B(k,N-k+1)} \\ &\quad \times [2\Phi(\gamma/\sqrt{x})-1]^{N-k} \\ &\quad \times 2^{k-1}[1-\Phi(\gamma/\sqrt{x})]^{k-1}\frac{\gamma}{\sqrt{2\pi}}\frac{1}{x^{3/2}}e^{-\gamma^2/2x}\,dx. \end{aligned} \tag{12}$$

By using the substitution $y = \gamma/\sqrt{x}$, the P_{fa} can be expressed as

$$\begin{aligned} P_{\mathrm{fa}} &= \frac{2^k}{\sqrt{2\pi}}\frac{1}{B(k,N-k+1)}\int_0^\infty [2\Phi(y/\sqrt{T})-1] \\ &\quad \times [2\Phi(y)-1]^{N-k}[1-\Phi(y)]^{k-1}e^{-y^2/2}\,dy. \end{aligned} \tag{13}$$

Finally, the false alarm probability can also be expressed as

$$\begin{aligned} P_{\mathrm{fa}}^{\mathrm{OS}} &= \sqrt{\frac{2}{\pi}}\frac{1}{B(k,N-k+1)}\int_0^\infty \mathrm{erf}(y/\sqrt{2T}) \\ &\quad \times [\mathrm{erf}(y/\sqrt{2})]^{N-k}[\mathrm{erfc}(y/\sqrt{2})]^{k-1}e^{-y^2/2}\,dy \end{aligned} \tag{14}$$

where

$$\mathrm{erf}(y) = \frac{2}{\sqrt{\pi}}\int_0^y e^{-t^2}\,dt \tag{15}$$

is the *error function*, $\text{erfc}(y) = 1 - \text{erf}(y)$ is the complementary error function, and it holds that

$$\Phi(y) = \tfrac{1}{2} + \tfrac{1}{2}\text{erf}(y/\sqrt{2}). \tag{16}$$

Equation (14) shows that the false alarm probability is controlled by the scaling factor T and it does not depend on the dispersion parameter γ of the Pearson-distributed parent population. Hence, the OS method is a CFAR method for Pearson background. Naturally, the use of OS does not define a single CFAR method but rather a family of CFAR methods parameterized by the rank order index k. For a given OS $X_{(k)}$, a distinct CFAR processor is established.

2) *Probability of Detection* P_d: We now compute the detection probability P_d of the OS CFAR detector. We consider the case of a Rayleigh fluctuating target in a heavy-tailed background noise scenario when the CFAR processor is preceded by a square-law detector, as in Fig. 1.

For a Rayleigh fluctuating target with parameter σ_s^2, the output of a square-law detector has an exponential pdf. Hence, for the case of the "target present" hypothesis, the test-cell measurement is exponentially distributed:

$$p_{Y_1}(y) = \begin{cases} \dfrac{1}{2\sigma_s^2} e^{-y/2\sigma_s^2}, & y \geq 0 \\ 0 & \text{otherwise} \end{cases}. \tag{17}$$

The corresponding cdf is

$$P_{Y_1}(y) = \Pr\{Y_1 \leq y\} = \begin{cases} 1 - e^{-y/2\sigma_s^2}, & y \geq 0 \\ 0 & \text{otherwise} \end{cases}. \tag{18}$$

Hence, the probability of the random variable Y_1 exceeding the threshold is

$$P_d = \Pr\{Y_1 \geq TX_{(k)}\}. \tag{19}$$

Assuming the presence of heavy-tailed clutter that leads to Pearson-distributed reference-cell data $X_1, \ldots, X_N$, the density of the kth OS is given by expression (11), and therefore P_d can be written as

$$\begin{aligned} P_d &= \int_0^\infty \Pr\{Y_1 \geq Tx\} p_k(x)\, dx \\ &= \int_0^\infty e^{-Tx/2\sigma_s^2} \frac{1}{B(k, N-k+1)} [2\Phi(\gamma/\sqrt{x}) - 1]^{N-k} \\ &\quad \times 2^{k-1}[1 - \Phi(\gamma/\sqrt{x})]^{k-1} \frac{\gamma}{\sqrt{2\pi}} \frac{1}{x^{3/2}} e^{-\gamma^2/2x}\, dx. \end{aligned} \tag{20}$$

Setting $y = \gamma/\sqrt{x}$, the final expression for the probability of detection of the OS CFAR processor can be written in terms of the error function as

$$\begin{aligned} P_d^{\text{OS}} &= \sqrt{\frac{2}{\pi}} \frac{1}{B(k, N-k+1)} \int_0^\infty e^{(-\gamma^2/\sigma_s^2)(T/2y^2)} \\ &\quad \times [\text{erf}(y/\sqrt{2})]^{N-k} [\text{erfc}(y/\sqrt{2})]^{k-1} e^{-y^2/2}\, dy. \end{aligned} \tag{21}$$

As we can see in (21), the detection probability is a function of the ratio of the clutter dispersion γ over the power parameter of the Rayleigh fluctuating target σ_s. To obtain the detection probability for a given probability of false alarm, one first has to solve (14) with respect to the required threshold, then substitute this value into (21) and numerically integrate the expression.

C. CA CFAR for Pearson-Distributed Data

The OS CFAR processor has been introduced as an improvement on the CA CFAR method, which selects the average of the reference cell values instead of the kth OS as a measure of the clutter level Z, i.e, $Z = (1/N)\sum_{i=1}^N X_i$. It is of interest to compare the P_{fa} of the two processors for the case of Pearson-distributed measurements. When using CA, Z is a Pearson-distributed random variable since it is the average sum of N Pearson-distributed random variables. The dispersion of Z is equal to $\gamma_Z = \sqrt{N}\gamma_{X_i}$. Hence, the pdf of Z is given by

$$p_Z(z) = \begin{cases} \dfrac{\sqrt{N}\gamma}{\sqrt{2\pi}} \dfrac{1}{z^{3/2}} e^{-N\gamma^2/2z}, & z \geq 0 \\ 0 & \text{otherwise} \end{cases}. \tag{22}$$

Then, using again (9), the P_{fa} can be expressed as

$$\begin{aligned} P_{fa} &= \Pr\{Y_0 \geq TZ\} \\ &= \int_0^\infty \Pr\{Y_0 \geq Tz\} p_Z(z)\, dz \\ &= \int_0^\infty [2\Phi(\gamma/\sqrt{Tz}) - 1] \frac{\sqrt{N}\gamma}{\sqrt{2\pi}} \frac{1}{z^{3/2}} \\ &\quad \times e^{-N\gamma^2/2z}\, dz. \end{aligned} \tag{23}$$

Setting $y = \gamma/\sqrt{x}$, we get

$$P_{fa}^{\text{CA}} = \sqrt{\frac{2N}{\pi}} \int_0^\infty \text{erf}(y/\sqrt{2T}) e^{-Ny^2/2}\, dy. \tag{24}$$

From (24) we see that CA is also a CFAR method for Pearson background. The corresponding probability of detection for the case of a Rayleigh target can be expressed as

$$\begin{aligned} P_d &= \Pr\{Y_1 \geq TZ\} \\ &= \int_0^\infty \Pr\{Y_1 \geq Tz\} p_Z(z)\, dz \\ &= \int_0^\infty e^{-Tz/2\sigma_s^2} \frac{\sqrt{N}\gamma}{\sqrt{2\pi}} \frac{1}{z^{3/2}} e^{-N\gamma^2/2z}\, dz \end{aligned} \tag{25}$$

and finally as

$$P_{\rm d}^{\rm CA} = \sqrt{\frac{2N}{\pi}} \int_0^{\infty} e^{(-\gamma^2/\sigma_s^2)(T/2y^2)} e^{-Ny^2/2} dy. \quad (26)$$

We see again that the detection probability is a function of the ratio of the clutter dispersion γ over the power parameter of the Rayleigh fluctuating target σ_s.

D. P-percent Truncated Mean Detector

As mentioned in the previous sections, both the CA and OS schemes determine the adaptive threshold by estimating the noise level from the data in the reference window. The CA detector uses a procedure based on the data sample mean, while the OS detector uses the kth ordered statistic value, which is more robust to the presence of undesired outliers in the data. In the following, we analyze the performance of another CFAR detector that is robust in the presence of heavy-tailed measurements. The so-called PTM processor is defined as the arithmetic mean of the first p-percent of the ranked observations. This type of detector is also known as the *censored mean-level detector* and it has been proposed as a CFAR solution to nonhomogeneous backgrounds [3, 4] arising in the presence of clutter edges or multiple targets.

1) *PTM CFAR for Pearson-Distributed Data*: We now compute the $P_{\rm fa}$ to show that the PTM is a CFAR method in the presence of Pearson-distributed data. Let us consider again the N IID data samples $X_1, X_2, \ldots, X_N$ of the reference cells and let $W_1, W_2, \ldots, W_{N-p}$ be the remaining set of variables upon censoring the p largest X_k, $k = 1, \ldots, N$. The PTM detector calculates the clutter level Z by averaging samples $W_1, W_2, \ldots, W_{N-p}$:

$$Z = \frac{1}{N-p} \sum_{k=1}^{N-p} W_k. \quad (27)$$

To determine the pdf of Z, we proceed as follows. Since the reference samples $X_1, \ldots, X_N$ are IID, the remaining samples $W_1, \ldots, W_{N-p}$ are also IID random variables whose common density $h_p(w)$ we have to determine. From the analysis of the OS CFAR detector, recall that the kth ordered sample, $X_{(k)}$ (out of N IID samples) has a pdf as in (10)

$$p_{X_{(k)}}(w) = p_k(w) = k \binom{N}{k} [1 - P_X(w)]^{N-k} \times [P_X(w)]^{k-1} p_X(w) \quad (28)$$

where $p_X(w)$ and $P_X(w)$ are, respectively, the pdf and the cdf of each one of the N IID random variables prior to the ranking. Since a single W_k is equally likely to have any rank from 1 to $N-p$, the common density $h_p(w)$ can be obtained by averaging (28) over the uniform distribution of the rank k [4]

$$h_p(w) = \frac{1}{N-p} \sum_{k=1}^{N-p} p_k(w). \quad (29)$$

It also holds that

$$p_X(w) = \frac{1}{N} \sum_{k=1}^{N} p_k(w) = \frac{N-p}{N} h_p(w) + \frac{1}{N} \sum_{k=N-p+1}^{N} p_k(w). \quad (30)$$

Solving for $h_p(w)$, we obtain

$$\begin{aligned} h_p(w) &= \frac{N}{N-p} p_X(w) - \frac{1}{N-p} \sum_{k=N-p+1}^{N} p_k(w) \\ &= \frac{N}{N-p} p_X(w) - \frac{1}{N-p} \sum_{k=N-p+1}^{N} k \binom{N}{k} \\ &\quad \times [1 - P_X(w)]^{N-k} [P_X(w)]^{k-1} p_X(w) \\ &= \frac{N}{N-p} p_X(w) \left[1 - \frac{1}{N} \sum_{k=N-p+1}^{N} \frac{N!}{(N-k)!(k-1)!} \right. \\ &\quad \left. \times [1 - P_X(w)]^{N-k} [P_X(w)]^{k-1} \right]. \end{aligned} \quad (31)$$

Using (6), (7), and (16), the expression for $h_p(w)$ can be written as

$$\begin{aligned} h_p(w) &= \frac{N}{N-p} \frac{\gamma}{\sqrt{2\pi}} \frac{1}{w^{3/2}} e^{-\gamma^2/2w} \\ &\quad \times \left[1 - \frac{1}{N} \sum_{k=N-p+1}^{N} \frac{N!}{(N-k)!(k-1)!} \right. \\ &\quad \left. \times (\mathrm{erf}(\gamma/\sqrt{2w}))^{N-k} (1 - \mathrm{erf}(\gamma/\sqrt{2w}))^{k-1} \right]. \end{aligned} \quad (32)$$

By expanding the factor $(1 - \mathrm{erf}(\gamma/\sqrt{2w}))^{k-1}$, $h_p(w)$ can be written as

$$\begin{aligned} h_p(w) &= \frac{1}{N-p} \frac{\gamma}{\sqrt{2\pi}} \frac{1}{w^{3/2}} e^{-\gamma^2/2w} \\ &\quad \times \left[N - \sum_{k=N-p+1}^{N} \sum_{j=0}^{k-1} \frac{N!}{(N-k)!(k-1)!} \binom{k-1}{j} \right. \\ &\quad \left. \times (-1)^j (\mathrm{erf}(\gamma/\sqrt{2w}))^{N-k+j} \right]. \end{aligned} \quad (33)$$

The corresponding characteristic function is

$$\varphi_p(\tau) = \frac{1}{N-p}\frac{\gamma}{\sqrt{2\pi}}\int_0^\infty \frac{1}{w^{3/2}}e^{-\gamma^2/2w}$$
$$\times\left[N - \sum_{k=N-p+1}^{N}\sum_{j=0}^{k-1}\frac{N!}{(N-k)!(k-1)!}\binom{k-1}{j}\right.$$
$$\left.\times(-1)^j(\mathrm{erf}(\gamma/\sqrt{2w}))^{N-k+j}\right]e^{j\tau w}dw. \quad (34)$$

By applying the substitution $t = \gamma/\sqrt{2w}$, we have

$$\varphi_p(\tau) = \frac{1}{N-p}\frac{2}{\sqrt{\pi}}\int_0^\infty e^{-t^2}$$
$$\times\left[N - \sum_{k=N-p+1}^{N}\sum_{j=0}^{k-1}\frac{N!}{(N-k)!(k-1)!}\binom{k-1}{j}\right.$$
$$\left.\times(-1)^j(\mathrm{erf}(t))^{N-k+j}\right]e^{j(\tau\gamma^2/2t^2)}dt$$
$$= g(\tau\gamma^2/2). \quad (35)$$

Including the factor $1/(N-p)$ in the scaling factor T, the pdf of Z is determined as the pdf of a random variable resulting from the sum of $N-p$ IID random variables having characteristic function $\varphi_p(\tau)$. Therefore,

$$p_Z(z) = \frac{1}{2\pi}\int_{-\infty}^{\infty}[\varphi_p(\tau)]^{N-p}e^{-j\tau z}d\tau. \quad (36)$$

We can now compute the P_{fa} as

$$P_{\mathrm{fa}}^{\mathrm{PTM}} = \Pr\{Y_0 \geq TZ\} = \int_0^\infty \Pr\{Y_0 \geq Tz\}p_Z(z)dz$$
$$= \int_0^\infty \mathrm{erf}(\gamma/\sqrt{2Tz})\frac{1}{2\pi}\int_{-\infty}^{\infty}[\varphi_p(\tau)]^{N-p}e^{-j\tau z}d\tau dz. \quad (37)$$

Recalling (36) and substituting $\nu = \tau\gamma^2/2$, we obtain

$$P_{\mathrm{fa}}^{\mathrm{PTM}} = \frac{1}{2\pi}\frac{2}{\gamma^2}\int_0^\infty \mathrm{erf}(\gamma/\sqrt{2Tz})$$
$$\times\int_{-\infty}^{\infty}[g(\nu)]^{N-p}e^{-j(2\nu z/\gamma^2)}d\nu dz \quad (38)$$

and with a last change of variables $q = 2z/\gamma^2$, we have

$$P_{\mathrm{fa}}^{\mathrm{PTM}} = \frac{1}{2\pi}\int_0^\infty \mathrm{erf}(1/\sqrt{Tq})\int_{-\infty}^{\infty}[g(\nu)]^{N-p}e^{-j\nu q}d\nu dq. \quad (39)$$

From (39), we notice that the PTM method is CFAR on Pearson background, since the P_{fa} does not depend on the dispersion parameter γ.

Considering the Rayleigh fluctuating target model, we now find an expression for the probability of detection P_{d}. By definition,

$$P_{\mathrm{d}} = \Pr\{Y_1 \geq TZ\} = \int_0^\infty \Pr\{Y_1 \geq Tz\}p_Z(z)dz \quad (40)$$

which, using (18) and (36), becomes

$$P_{\mathrm{d}}^{\mathrm{PTM}} = \int_0^\infty e^{-Tz/2\sigma_s^2}\frac{1}{2\pi}\int_{-\infty}^{\infty}[\varphi_p(\tau)]^{N-p}e^{-j\tau z}d\tau dz$$
$$= \int_0^\infty e^{-(T\gamma^2/4\sigma_s^2)q}\int_{-\infty}^{\infty}[g(\nu)]^{N-p}e^{-j\nu q}d\nu dq. \quad (41)$$

We can see from this expression that the P_{d} is controlled by the ratio of the clutter dispersion γ and the power of the fluctuating target σ_s.

III. RESULTS AND DISCUSSION

In this section, the detection performance of the OS CFAR processor in Pearson-distributed data in homogeneous situations is shown and compared with the performance of the CA CFAR detector. The detection performances are obtained by varying the number of the reference cells N and, for the case of the OS CFAR processor, the rank order index k. For a certain P_{fa} value, we used expressions (14) and (24) to obtain the appropriate threshold scaling factors T for the OS and CA detectors, respectively. Then, we numerically integrated (21) and (26) to calculate the corresponding P_{d} values.

In Fig. 2 the probability of detection P_{d} is plotted versus the generalized signal-to-noise ratio (GSNR) for probability of false alarm $P_{\mathrm{fa}} = 10^{-4}$. The GSNR is defined as

$$\mathrm{GSNR} = 20\log\frac{\sigma_s}{\gamma} \quad (42)$$

where σ_s is the parameter of the Rayleigh fluctuating target and γ is the dispersion parameter of the Pearson-distributed output of the square-law detector due to the background heavy-tailed clutter. This definition of relative strength between signal and noise is well motivated from expressions (21) and (26), which give the detection probabilities as functions of the ratio σ_s/γ.

We should note here that although the moment EX^2 of a second-order process has been widely accepted as a standard measure of signal strength and associated with the physical concept of power and energy, it cannot be used with alpha-stable distributions because it is infinite. Hence, the GSNR expression in (42) should not be interpreted as a signal to noise *power* ratio.

Focusing our attention to the ROC curves in Fig. 2, it can be seen that for high GSNR values (GSNR > 75 dB), the detection performance of the OS CFAR processor is better for smaller values of

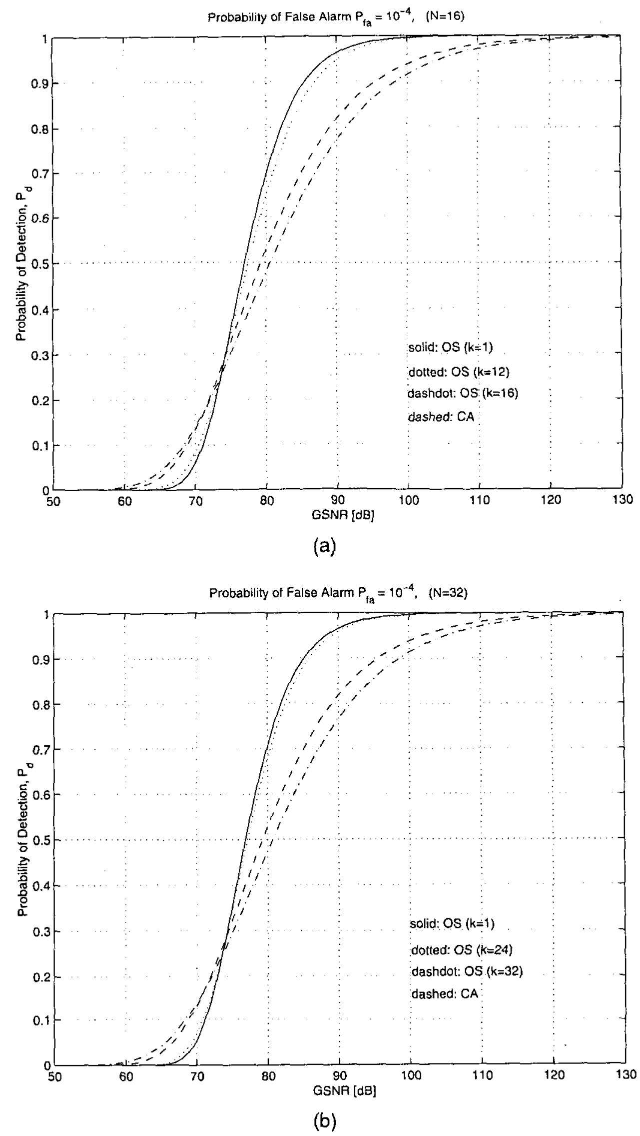

Fig. 2. Detection probability of OS and CA CFAR processors in Pearson background as function of GSNR = $20\log(\sigma_s/\gamma)$. Reference window size is $N = 16$ (a) and $N = 32$ (b). Probability of false alarm equal to $P_{fa} = 10^{-4}$.

the rank order index k. On the other hand, for low GSNR values, the detection performance of the OS CFAR processor is better for larger values of the rank order index k. As a middle ground rank order, the value of $k = 3N/4$ seems to result in only a negligible additional CFAR loss. The detection performance of the CA CFAR processor is also shown in the figures with a dashed line. It is apparent that for an appropriate choice of the rank order index k, the corresponding OS CFAR processor outperforms CA CFAR for the case of homogeneous Pearson-distributed background clutter.

Fig. 3 depicts the ROC curves for the OS and CA CFAR processors employing $N = 16$ reference cells and operating in GSNR equal to 70 dB, 90 dB, and 110 dB. We see that, for an GSNR value of 70 dB and for the range of P_{fa} values between 1.5×10^{-4} to 10^{-2}, the OS CFAR processor employing the first-order statistic (minimum) of the reference cells exhibits the best performance. On the other hand, for P_{fa} values less than 1.5×10^{-4}, the other extremum, i.e., the last-order statistic (maximum) of the reference cells has the best P_d. Similar observations can be made for the case of the other operating GSNR values for the corresponding P_{fa}. Again, the performance curve of the CA CFAR processor falls in between the OS family of curves, and a good compromise OS corresponds to a value of k equal to $3N/4$. Finally, we see that as the GSNR value decreases, the shape of the ROC curves stays the same but the performance curves move to the right towards higher P_{fa} values, as expected.

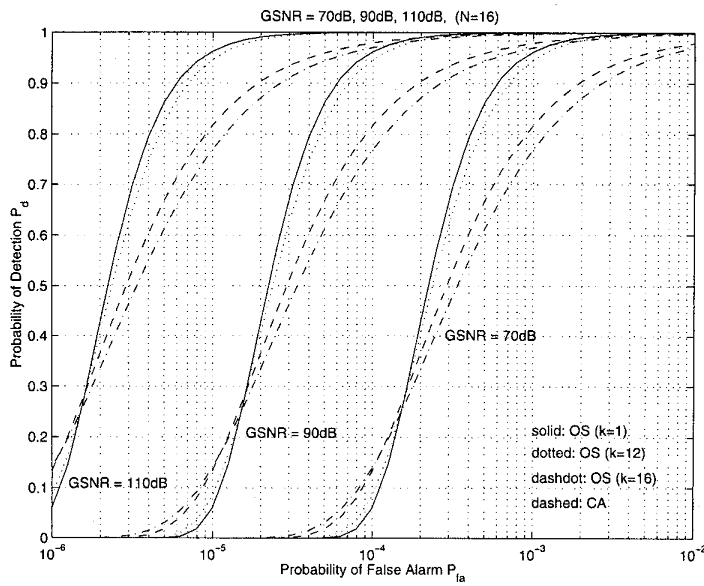

Fig. 3. ROC: Detection probability of OS and CA CFAR processors in Pearson background versus probability of false alarm, for various GSNR values.

IV. FUTURE WORK

In this work, we presented a theoretical analysis on the performance of the OS, CA, and PTM CFAR processors for the case of Pearson-distributed data. The implications of this work for real life CFAR systems operating in severe noise environments such as the ones described and modeled by Pierce in [10], is that the threshold that must be employed to achieve a certain probability of detection and to ensure a constant probability of false alarm has to be set at a higher value than what is assumed under previous studies.

When the characteristic exponent of the $P\alpha S$ distribution is unknown, a two-parameter estimation CFAR algorithm is needed. The adaptive threshold will effectively be based on the estimation of the scale (dispersion) and shape (characteristic exponent) parameters using the method of negative-order moments proposed by Pierce in [10].

In addition to the CFAR processors studied here, one may design receivers targeted to operate in non-Gaussian noise characterized by heavy tails. Usually, these receivers consist of a limiting device, followed by a correlation detector. An example is coherent detection in IID Laplacian noise, where the optimum detector soft-limits the data and then correlates the soft-limited observations with the sequence of signal signs [15, pp. 49–51]. Recently, we have introduced detectors and estimators for alpha-stable impulsive noise with promising results. In particular, we designed optimum maximum likelihood based estimators, which operate in Cauchy distributed noise [16]. Optimal detectors have also been designed and it has been shown that they perform better than the limiter plus integrator receiver [17]. As shown in [18], instead of a correlation operation, the so-called covariation computation has a "limiting device" inherent into it and gives better results in impulsive noise.

PANAGIOTIS TSAKALIDES
VLSI Design Laboratory
Department of Electrical and Computer Engineering
University of Patras
261 10 Rio, Greece
E-mail: (tsakalid@ee.upatras.gr)

FLIPPO TRINCI
WIND Telecomunicazioni S.p.A.
NETWORK–Access Networks
Rome, Italy
E-mail: (ftrinci@wind.it)

CHRYSOSTOMOS L. NIKIAS
Integrated Media Systems Center
Department of Electrical Engineering
University of Southern California
Los Angeles, CA 90089-2561
E-mail: (nikias@imsc.usc.edu)

REFERENCES

[1] Gandhi, P. P., and Kassam, S. A. (1988)
Analysis of CFAR processors in nonhomogeneous background.
IEEE Transactions on Aerospace and Electronic Systems, **24** (1988), 427–445.

[2] Rohling, H. (1983)
Radar CFAR thresholding in clutter and multiple target situations.
IEEE Transactions on Aerospace and Electronic Systems, **AES-19** (1983), 608–621.

[3] Rickard, J. T., and Dillard, G. M. (1977)
Adaptive detection algorithms for multiple-target situations.
IEEE Transactions on Aerospace and Electronic Systems, **AES-13** (July 1977).

[4] Ritcey, J. A. (1986)
Performance analysis of the censored mean level detector.
IEEE Transactions on Aerospace and Electronic Systems, **AES-22** (July 1986).

[5] Tsakalides, P., Raspanti, R., and Nikias, C. L. (1999)
Angle/Doppler estimation in heavy-tailed clutter backgrounds.
IEEE Transactions on Aerospace and Electronic Systems, **35** (Apr. 1999), 419–436.

[6] Pierce, R. D. (1996)
RCS characterization using the alpha-stable distribution.
In *Proceedings of the IEEE National Radar Conference* (May 1996), 154–159.

[7] Conte, E., Lops, M., and Tulino, A. M. (1997)
Hybrid procedure for CFAR in non-Gaussian clutter.
IEE Proceedings, Radar, Sonar and Navigation, **144** (Dec. 1997), 361–369.

[8] Weber, P., and Haykin, S. (1985)
Ordered statistics CFAR for two-parameter distributions with variable skewness.
IEEE Transactions on Aerospace and Electronic Systems, **AES-21** (1985), 819–821.

[9] Ravid, R., and Levanon, N. (1992)
Maximum likelihood CFAR for Weibull background.
IEE Proceedings, Pt. F, **139** (June 1992), 256–264.

[10] Pierce, R. D. (1997)
Application of the positive alpha-stable distribution.
In *IEEE Signal Processing Workshop on Higher-Order Statistics*, Banff, Alberta, Canada, July 21–23, 1997, 420–424.

[11] Tsakalides, P., and Nikias, C. L. (1999)
Robust space-time adaptive processing (STAP) in non-Gaussian clutter environments.
IEE Proceedings, Radar, Sonar, Navigation, **146** (Apr. 1999), 84–94.

[12] Samorodnitsky, G., and Taqqu, M. S. (1994)
Stable Non-Gaussian Random Processes: Stochastic Models with Infinite Variance.
New York: Chapman and Hall, 1994.

[13] Nikias, C. L., and Shao, M. (1995)
Signal Processing with Alpha-Stable Distributions and Applications.
New York: Wiley, 1995.

[14] Castillo, E. (1988)
Extreme Value Theory in Engineering.
San Diego, CA: Academic Press, 1988.

[15] Poor, H. V. (1994)
An Introduction to Signal Detection and Estimation (2nd ed.).
New York: Springer, 1994.

[16] Tsakalides, P., and Nikias, C. L. (1995)
Maximum likelihood localization of sources in noise modeled as a stable process.
IEEE Transactions on Signal Processing, **43** (Nov. 1995), 2700–2713.

[17] Tsihrintzis, G. A., and Nikias, C. L. (1995)
Performance of optimum and suboptimum receivers in the presence of impulsive noise modeled as an alpha-stable process.
IEEE Transactions on Communication, **43** (Mar. 1995), 904–914.

[18] Tsakalides, P., and Nikias, C. L. (1996)
The robust covariation-based MUSIC (ROC-MUSIC) algorithm for bearing estimation in impulsive noise environments.
IEEE Transactions on Signal Processing, **44** (July 1996), 1623–1633.

2D Model-Based Step-Track Procedure

A 2D model-based generalization of the gradient step-track is introduced and simulation results are presented showing an overall tracking accuracy improvement and limit signal-to-noise ratio (SNR) advantage over the hill-climbing and the gradient procedures. At best, the new method is shown to allow a worse than 20 dB SNR in tracking a near geosynchronous satellite.

I. INTRODUCTION

Tracking methods based on signal level measurements between small angular step displacements of the parabolic receiving antenna are widely used in low grade earth station systems of near geosynchronous satellites and also as a back-up in high-grade systems [1, 2].

Hill-climbing method seeks to maximize the signal level through iteration, where constant size angular steps are taken in orthogonal coordinate directions in turn, and the decision about the sign of the next step in one coordinate direction is made by comparing the levels before and after a step. Due to simple principle of operation, low cost implementation is possible, but a modest tracking accuracy in noise must be contended with. Increasing step size increases reliability of stepping decisions, but the benefit is paid with increasing disturbance of the traffic signal by the stepping process itself. Therefore a sufficient number of moderate size steps per activation gives best results [3, 5].

Hill-climbing system does not require direction angle transducers, but if the antenna system is able to measure beam direction angles between step turns, algorithms are available, which better utilize the known dependence of the received level on pointing error. For operation near the beam axis holds

$$L(x,y) \approx K_x(x-p)^2 + K_y(y-q)^2 + L_{pq} \qquad (1)$$

where (x,y) is the angular direction of the beam axis, $L(x,y)$ is the corresponding level in dB of the received signal, (p,q) is the angular direction of the satellite, and L_{pq} is level at zero pointing error. K_x and K_y are structural constants specifying the steepness of the

Manuscript received April 28, 1996; revised January 5 and July 5, 2000; released for publication July 5, 2000.

IEEE Log No. T-AES/36/4/11384.

Refereeing of this contribution was handled by X. R. Li.

This work was partly supported by the Technical Research Centre of Finland and the Helsinki University of Technology.

0018-9251/00/$10.00